Chinese Chemical Letters 31 (2020) 554–558

Contents lists available at ScienceDirect

Chinese Chemical Letters

journal homepage: www.elsevier.com/locate/cclet

Communication

Thermal studies of novel molecular perovskite energetic material $(C_6H_{14}N_2)[NH_4(ClO_4)_3]$

Jing Zhou[a], Li Ding[a,*], Fengqi Zhao[a], Bozhou Wang[a], Junlin Zhang[a,b,*]

[a] Xi'an Modern Chemistry Research Institute, Xi'an 710065 China
[b] Department of Chemistry, Technische Universität München, Garching bei München 85748, Germany

ARTICLE INFO

Article history:
Received 27 February 2019
Received in revised form 4 May 2019
Accepted 6 May 2019
Available online 6 May 2019

Keywords:
Cage skeleton
DSC-TG
In-situ FTIR
Inorganic-organic framework material
Thermal behaviors

ABSTRACT

$(C_6H_{14}N_2)[NH_4(ClO_4)_3]$ is a newly developed porous hybrid inorganic-organic framework material with easy access and excellent detonation performances, however, its thermal properties is still unclear and severely hampered further applications. In this study, thermal behaviors and non-isothermal decomposition reaction kinetics of $(C_6H_{14}N_2)[NH_4(ClO_4)_3]$ were investigated systematically by the combination of differential scanning calorimetry (DSC) and simultaneous thermal analysis methods. *In-situ* FTIR spectroscopy technology was applied for investigation of the structure changes of $(C_6H_{14}N_2)[NH_4(ClO_4)_3]$ and some selected referents for better understanding of interactions between different components during the heating process. Experiment results indicated that the novel molecular perovskite structure renders $(C_6H_{14}N_2)[NH_4(ClO_4)_3]$ better thermal stability than most of currently used energetic materials. Under high temperatures, the stability of the cage skeleton constructed by NH_4^+ and ClO_4^- ions determined the decomposition process rather than organic moiety confined in the skeleton. The simple synthetic method, good detonation performances and excellent thermal properties make $(C_6H_{14}N_2)[NH_4(ClO_4)_3]$ an ideal candidate for the preparation of advanced explosives and propellants.

Design new structures with superior performances is a foremost goal in the research of energetic materials [1,2]. Over the past decades, main strategies focused on the development of new organic energetic structures with more explosophores and higher strain energies, such as hexanitrohexaazaisowurtzitane (CL-20) [3], nitroadamantanes [4] and octanitrocubane (ONC) [5]. However, the complicated preparations severely hindered their applications in advanced explosives or propellants. More recently, energetic metal-organic frameworks (MOFs), porous crystalline energetic materials with ordered pores and channels, were achieved as another efficient approach through the combination of inorganic metal ions with organic energetic ligands (Fig. 1) [6–9]. Although the structure of energetic MOFs, especially energetic 3D MOF, provided unique architectural platforms for development of new-generation energetic materials, pre-synthesis of the complicated organic ligands is still essential.

From design perspective, energetic materials need to be both a fuel and oxidizer [10]. Most traditional energetic materials are compact organic structures with high densities, which include both the fuel (carbons in the molecular skeletons) and oxidizer (oxygen on the nitro groups) moieties within the same molecule [11]. In contrast, energetic mixtures formed by simply mixing the fuel and oxidizer components together always results in low density and slow reaction rates limited by mass-transfer rates, which further lead to poor detonation performances. $(C_6H_{14}N_2)[NH_4(ClO_4)_3]$ is a new molecular perovskite energetic material consisting of protonated 1,4-diazabicyclo[2.2.2]octane (DABCO), inorganic cation (NH_4^+) and anion (ClO_4^-) [12]. Its fuel and oxidizer components are combined in appropriate ratio and close distance, which leads to high energetic density level, sufficient combustion and rapid detonation (Fig. 2). Moreover, the synthesis of $(C_6H_{14}N_2)[NH_4(ClO_4)_3]$ can be achieved by simply mixing DABCO, NH_4ClO_4 and $HClO_4$ in high yield. All these features are highly suitable for new-generation of advanced energetic material. However, its thermal properties, another key index on evaluating the quantity of energetic materials, are still unclear. Unlike traditional energetic structures, in $(C_6H_{14}N_2)[NH_4(ClO_4)_3]$, protonated DABCO is actually confined in a cubic anionic coordinated framework constructed by the oxidizing anions and reducing cations alternated with each other in the space. The distinctive protonated DABCO lock effect may result in entirely new thermal behaviors, which will also promote the understandings of this novel molecular perovskite energetic materials as well as their further applications in both military

* Corresponding authors at: Xi'an Modern Chemistry Research Institute, Xi'an, 710065, China.
E-mail addresses: dingli403@sina.com (L. Ding), junlin-111@163.com (J. Zhang).

https://doi.org/10.1016/j.cclet.2019.05.008
1001-8417/

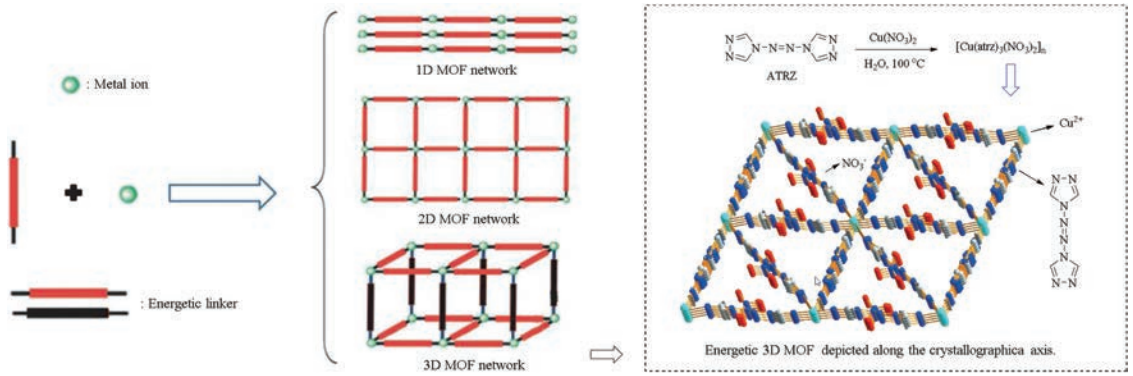

Fig. 1. Energetic MOFs structures [6].

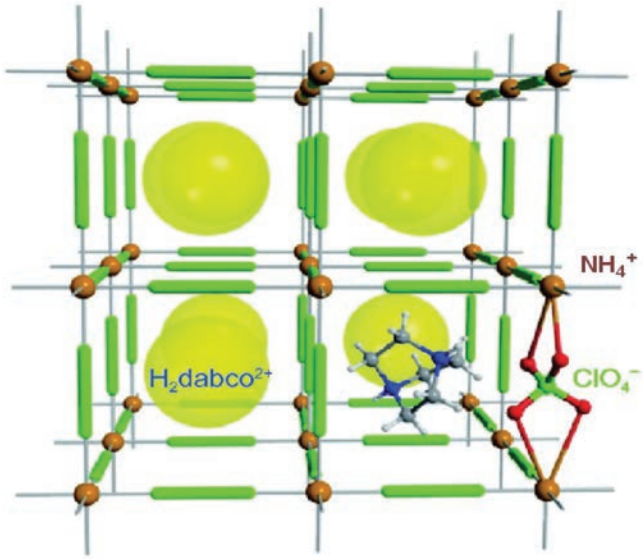

Fig. 2. Structure of $(C_6H_{14}N_2)[NH_4(ClO_4)_3]$ [12].

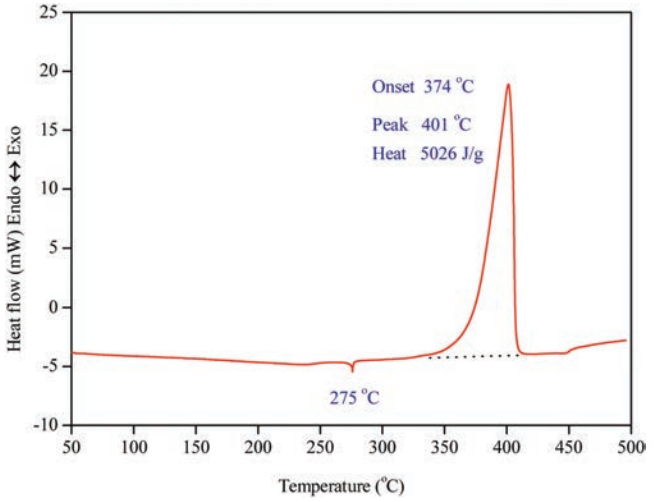

Fig. 3. DSC curve of $(C_6H_{14}N_2)[NH_4(ClO_4)_3]$ at the heating rate of 10 °C/min.

equipment and civil industry. Herein, we reported the first systematic research on thermal behaviors and the non-isothermal decomposition reaction kinetics of $(C_6H_{14}N_2)[NH_4(ClO_4)_3]$ by the combination of differential scanning calorimetry (DSC) and simultaneous thermal analysis methods. *In-situ* FTIR spectroscopy technologies were also applied for the investigation of the interactions between different components in the material and the structure changes of the framework during the pyrolysis process.

Detailed studies on thermal decomposition behaviors was first carried out. From practical point of view, thermal decomposition behaviors deeply affect the quality of an energetic material and its shelf life, as well as its thermal hazard potential. Therefore, thermal decomposition behaviors are always regarded as a key index on evaluating the quantity of new energetic materials [13–15]. The thermal behaviors of $(C_6H_{14}N_2)[NH_4(ClO_4)_3]$ were first investigated through DSC measurements and there is no thermal change observed until a endothermic peak appeared at 275 °C (Fig. 3). The sample showed no signs of melting at this temperature and the endothermic peak was extremely weak, which means this endothermic process was more likely to be caused by the change of crystalline form rather than a melting or organic moiety extrusion process. The rotation of the organic moiety inside the cage skeleton may trigger the change of crystalline form. DSC experiment showed that thermal decomposition of $(C_6H_{14}N_2)[NH_4(ClO_4)_3]$ was a one-step process at the temperature range 50~500 °C. The decomposition temperature of $(C_6H_{14}N_2)[NH_4(ClO_4)_3]$ at the heating rate of 10 °C/min was around 400 °C, much higher than those of the famous single explosives such RDX, HMX, HNAB and CL-20 under similar heating conditions [16,17] (Table 1). 5026 J/g of heat was released during the thermal decomposition of $(C_6H_{14}N_2)[NH_4(ClO_4)_3]$, which was even larger than heat release of the most powerful high explosives like HMX (1987 J/g) and CL-20 (3101 J/g) [18]. Moreover, the heat release of $(C_6H_{14}N_2)[NH_4(ClO_4)_3]$ was highly concentrated, indicated a powerful energy release capacity.

Strong and special interactions were existed between protonated DABCO, NH_4^+ and ClO_4^- in $(C_6H_{14}N_2)[NH_4(ClO_4)_3]$, which could be clearly proved through DSC experiments. For better understanding of these interactions during the heating process, DSC analysis of DABCO-AP mixture, which contained similar ion components as $(C_6H_{14}N_2)[NH_4(ClO_4)_3]$, was carried out with the result showed in Fig. 4. The DSC curve of DABCO-AP mixture demonstrated that the thermal behavior of the mixture was more like a combination of

Table 1
Decomposition temperature of $(C_6H_{14}N_2)[NH_4(ClO_4)_3]$ compared with some traditional explosives.

	$(C_6H_{14}N_2)[NH_4(ClO_4)_3]$	RDX	HMX	CL-20	HNAB
T_p[a]	401 °C	210 °C	283 °C	244 °C	220 °C

[a] T_p is decomposition peak temperature.

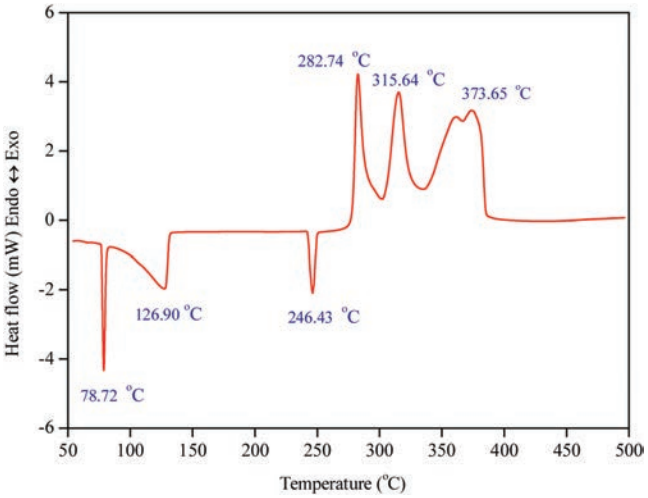

Fig. 4. DSC curve of DABCO-AP mixture at the heating rate of 10 °C/min.

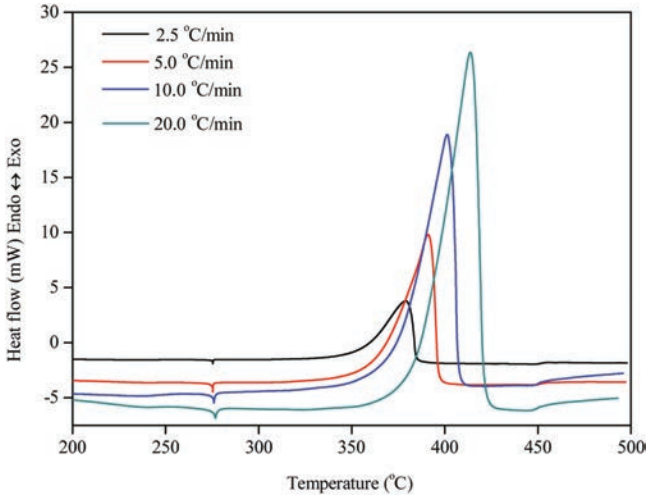

Fig. 6. DSC curves of $(C_6H_{14}N_2)[NH_4(ClO_4)_3]$ at different heating rates.

DABCO and AP by comparation with the reported endothermic and exothermic peaks of DABCO and AP [19,20]. Obviously, the energy-released process of $(C_6H_{14}N_2)[NH_4(ClO_4)_3]$ was much more concentrate as a single compound.

Further studies were carried out through TG/DTG approach. Single weight loss process was found in TG curve and the peak temperature in DTG curve of $(C_6H_{14}N_2)[NH_4(ClO_4)_3]$ coincided well with the decomposition peak temperature from the DSC experiment. No weight loss was observed before the decomposition process, indicating the weak endothermic peak appeared around 275 °C on DSC curve of $(C_6H_{14}N_2)[NH_4(ClO_4)_3]$ was not caused by the extrusion of DABCO (Fig. 5).

Kinetic constants of the energetic materials are also important parameters for accurate prediction of the shelf-life and thermal hazard potential in their applications. The non-isothermal DSC measurements of $(C_6H_{14}N_2)[NH_4(ClO_4)_3]$ were carried out at different heating rates using samples with same mass. Clearly, faster heating rates yield higher peak temperatures while the peak height increases proportionally with the heating rate. As shown in Fig. 6, decomposition peak temperatures were 379 °C, 390 °C, 401 °C and 413 °C at the heating rates of 2.5 °C/min, 5 °C/min, 10 °C/min and 20 °C/min, respectively. The apparent activation energies and pre-exponential factors were determined by analysis of the DSC curves with Kissinger [21] and Ozawa [22] models. Table 2 summarized the kinetic results derived by the two models with good agreements and apparent activation energy of

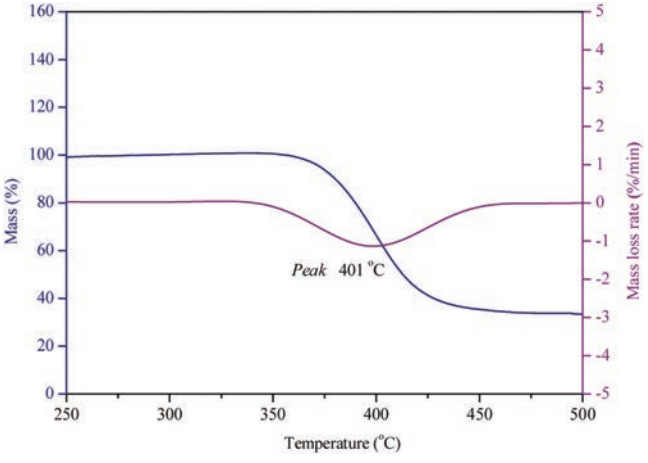

Fig. 5. TG/DTG curve of $(C_6H_{14}N_2)[NH_4(ClO_4)_3]$ at the heating rate of 10 °C/min.

$(C_6H_{14}N_2)[NH_4(ClO_4)_3]$ is around 215 kJ/mol, very close to the reported result of RDX (211 kJ/mol) [23].

Both the steady covalent bonds of organic moiety and structural reinforcement by strong Coulombic interactions between cations and anions in perovskite structure play important roles for the high thermal stability of $(C_6H_{14}N_2)[NH_4(ClO_4)_3]$. To clarify possible mechanism and interactions between different components during its thermal decomposition process, investigations of structure changes with raise of the temperatures were carried out through *in-situ* FTIR spectroscopy method. Viewed from structural perspective, $(C_6H_{14}N_2)[NH_4(ClO_4)_3]$ has similar cubic structure of the inorganic perovskites with a general formula of ABX_3 by regarding protonated DABCO as A-site cation, NH_4^+ as B-site cation and ClO_4^- as X-bridges. Distinguishing from most energetic salts derived from nitrogen-rich heterocycles and their cations, $(C_6H_{14}N_2)[NH_4(ClO_4)_3]$ was present a new class of single energetic compound with a cage skeleton constructed by inorganic cation and inorganic oxidizer anion while the organic cation (protonated DABCO) was confined in the cage (Fig. 2). Thermal stability of the material is determined by several key factors, including thermal stability of the cage skeleton, the organic component confined inside and their interactions.

DABCO confined in the cage skeleton acts as organic fuel in the energetic structure of $(C_6H_{14}N_2)[NH_4(ClO_4)_3]$. Curve a in Fig. S1 (Supporting information) showed the FTIR spectroscopy of DABCO at room temperature and signals located at 3427 cm^{-1} belonged to the amine moiety while signals located at 2944, 2876, 1459, 1320, 1060 and 778 cm^{-1} belonged to the methylene moieties. Compared the FTIR spectroscopy of DABCO at room temperature with that at 240 °C and 370 °C (curves b and c in Fig. S1), this organic component disappeared rapidly when heated to 240 °C through volatilization process and nothing left when heated to 370 °C. Further compared with the following experiment results of structure changes of $(C_6H_{14}N_2)[NH_4(ClO_4)_3]$ (Fig. S2 in Supporting information), the volatilization process no longer existed when the organic component was confined into the cage skeleton and the heating process did not lead to extrusion of DABCO from the hybrid inorganic-organic framework material.

The cage skeleton was constructed by NH_4^+ and ClO_4^- ions. For better understanding of the interactions between NH_4^+ and ClO_4^- ions in $(C_6H_{14}N_2)[NH_4(ClO_4)_3]$, AP was chosen as model system and investigated through *in-situ* FTIR spectroscopy. Curve a in Fig. S3 (Supporting information) showed FTIR spectascopy of AP at room temperature in which signals located at 3296 cm^{-1} belonged to the NH_4^+ group while 1404, 1083 and 626 cm^{-1} belonged to the ClO_4^-

Table 2
Thermal decomposition kinetic parameters of $(C_6H_{14}N_2)[NH_4(ClO_4)_3]$.

β (°C/min) [c]	T_p (K) [e]	ΔH (J/g)	*Kissinger*			*Ozawa*	
			Ea_1 (kJ/mol) [a]	lnA (s^{-1}) [d]	r	Ea_2 (kJ/mol) [b]	r
2.5	652	4888	215	33	0.9995	215	0.9995
5	664	5706					
10	674	5026					
20	686	5434					

[a] Ea_1 is the apparent activation energy (kJ/mol) obtained by Kissinger model.
[b] Ea_2 is the apparent activation energy (kJ/mol) obtained by Ozawa model.
[c] β is the heating rate.
[d] A is the pre-exponential factor (s^{-1}).
[e] T_p is the peak temperature (K).

group. Compared the FTIR spectascopy of AP at room temperature with its FTIR spectascopy at 240 °C, 370 °C and 400 °C (curves b–d in Fig. S3), following conclusions can be drawn: 1) No obvious structure change of AP could be observed at 240 °C; 2) The signals of AP began to disappear fast at 370 °C; 3) Most signals of AP could not be observed when the heating temperature was higher than 400 °C due to the decomposition process. The results indicated that the interaction between NH_4^+ and ClO_4^- ions was weak when the heating temperature was lower than 370 °C, with the further raise of the temperature, interactions between NH_4^+ and ClO_4^- ions became much stronger and the decomposition proceeded rapidly. Since the initial decomposition temperature of $(C_6H_{14}N_2)[NH_4(ClO_4)_3]$ at the heating rate of 10 °C/min is 374 °C, a temperature which is extremely close to the decomposition temperature of AP, it is highly probable that NH_4^+ and ClO_4^- ions in $(C_6H_{14}N_2)[NH_4(ClO_4)_3]$ has no interactions during the heating process until the temperature reached 370 °C.

Structure changes of $(C_6H_{14}N_2)[NH_4(ClO_4)_3]$ was investigated through *in-situ* FTIR spectroscopy based on the above studies (Fig. S2). From FTIR spectroscopy at room temperature, the overlap of signals from different components could be observed (curve a in Fig. S2) Signals located at 3000∼3500 cm^{-1} belonged to the amine moiety in protonated DABCO as well as the NH_4^+ group. Signals located at 1074 and 625 cm^{-1} belonged to the ClO_4^- group, while signals of methylene moieties in protonated DABCO were also located in this area and obscured by the broad strong signals of ClO_4^-. The signals of NH_4^+ and ClO_4^- groups stayed nearly unchanged until the temperature reached 370 °C (curve c in Fig. S2), while the signals of protonated DABCO began to weaken when the temperature was higher than 240 °C, which is probably caused by the change of the ring skeleton of DABCO (curve b in Fig. S2). However, there was no obvious exothermic process detected when the temperature was lower than 370 °C, which means no obvious interactions between the fuel and oxidative components (Fig. 3). Signal of $(C_6H_{14}N_2)[NH_4(ClO_4)_3]$ became very weak at 400 °C (curve d in Fig. S2) and nothing could be observed when the heating temperature reached 420 °C (curve e in Fig. S2). The experiments results of DSC and structure changes studies proved that the ring skeleton of protonated DABCO began to change first, while the cage skeleton of $(C_6H_{14}N_2)[NH_4(ClO_4)_3]$ stayed unchanged and confined the organic component inside when the temperature was lower than 370 °C. When the temperature was higher than 370 °C, strong oxidation of the organic component and NH_4^+ by ClO_4^- occurred, led to large amount of heat release. The raise of heating temperature weaken the skeleton of the organic component ahead of the cage skeleton of $(C_6H_{14}N_2)[NH_4(ClO_4)_3]$ and the organic component was still confined in the cage skeleton until the cage skeleton itself began to decompose. This confined effect of the inorganic cage skeleton rendered $(C_6H_{14}N_2)[NH_4(ClO_4)_3]$ super thermal stability which was different from traditional organic energetic materials.

In summary, thermal behaviors of newly developed molecular perovskite energetic material $(C_6H_{14}N_2)[NH_4(ClO_4)_3]$ was investigated through DSC-TG method as well as *in-situ* FTIR spectroscopy method. The experiment results showed the decomposition temperature of $(C_6H_{14}N_2)[NH_4(ClO_4)_3]$ was around 400 °C, which was much higher than most of the currently used energetic materials. Considerable amount of heat was generated in a concentrated way during the thermal decomposition process. *In-situ* FTIR spectroscopy experiments indicated that the stability of the cage skeleton constructed by NH_4^+ and ClO_4^- ions determined the decomposition process. The organic component of protonated DABCO was locked in the cage skeleton and the heating did not lead to extrusion of DABCO from the hybrid inorganic-organic framework material. When the temperature reached 370 °C, DABCO was released from the cubic cage and oxidized by the ClO_4^-. This confined effect from the inorganic cage skeleton rendered $(C_6H_{14}N_2)[NH_4(ClO_4)_3]$ super thermal stability which was different from traditional organic energetic materials.

Caution!

The described compounds are energetic materials with sensitivity to various stimuli. While we encountered no issues in the handling of these materials, proper protective measures should be used at all times.

Acknowledgments

This work was supported by the National Natural Science Foundation of China (Nos. 21805226 and 21805223), the China Postdoctoral Science Foundation (No. 2018M633552) and China Scholarship Council (No. 201805290006).

Appendix A. Supplementary data

Supplementary material related to this article can be found, in the online version, at doi:https://doi.org/10.1016/j.cclet.2019.05.008.

References

[1] C. Zhang, C.G. Sun, B.C. Hu, C.M. Yu, M. Lu, Science 355 (2017) 374–376.
[2] J.H. Zhang, L.A. Mitchell, D.A. Parrish, J.M. Shreeve, J. Am. Chem. Soc. 137 (2015) 10532–10535.
[3] L. Ding, F.Q. Zhao, Q. Pan, X.H. Xu, J. Anal. Appl. Pyrol. 121 (2016) 121–127.
[4] J. Zhang, T.J. Hou, L. Zhang, J. Luo, Org. Lett. 20 (2018) 7172–7176.
[5] M.X. Zhang, P.E. Eaton, R. Gilardi, Angew. Chem. Int. Ed. 39 (2000) 401–404.
[6] Q.H. Zhang, J.M. Shreeve, Angew. Chem. Int. Ed. 53 (2014) 2540–2542.
[7] B. Wu, L. Yang, S. Wang, et al., Z. Anorg. Allg. Chem. 637 (2011) 450–455.
[8] O.S. Bushuyev, P. Brown, A. Maiti, et al., J. Am. Chem. Soc. 134 (2012) 1422–1425.
[9] S.H. Li, Y. Wang, C. Qi, et al., Angew. Chem. Int. Ed. 125 (2013) 14031–14035.
[10] A. Sikder, N. Sikder, J. Hazard. Mater. 112 (2004) 1–15.
[11] X.X. Zhao, S.H. Li, Y. Wang, et al., J. Mater. Chem. A 4 (2016) 5495–5504.

[12] S.L. Chen, Z.R. Yang, B.J. Wang, et al., Sci. China Mater. 61 (2018) 1123–1128.
[13] J. Zhou, L. Ding, F.Q. Bi, B.Z. Wang, J.L. Zhang, J. Anal. Appl. Pyrol. 129 (2018) 189–194.
[14] T. An, W. He, S.W. Chen, et al., J. Phys. Chem. C 122 (2018) 26956–26964.
[15] B. Yan, H.Y. Li, Y.L. Guan, et al., Propell. Explos. Pyrot. 42 (2017) 382–1386.
[16] Q.L. Yan, S. Zeman, A. Elbeih, Z.W. Song, J. Málek, J. Therm. Anal. Calorim. 112 (2013) 823–836.
[17] J. Zhang, J. Wang, H.F. Xu, X.L. Zhou, Chin. J. Energy Mater. 21 (2013) 7–11.
[18] G.Q. Wang, L.B. Yang, H.L. Lu, et al., J. Solid. Rock. Technol. 40 (2017) 70–75.
[19] Z.R. Liu, C.M. Yin, Y.H. Kong, et al., Chin. J. Energy Mater. 8 (2000) 75–79.
[20] V.V. Boldyrev, Thermochim. Acta 443 (2006) 1–36.
[21] T.L. Zhang, R.Z. Hu, Y. Xie, F.P. Li, Thermochim. Acta 244 (1994) 171–176.
[22] L. Xue, F.Q. Zhao, R.Z. Hu, H.X. Gao, J. Energy Mater. 28 (2010) 17–34.
[23] E. Mohamed, E. Ahmed, H. Saeed, Cent. Eur. J. Energy Mater. 13 (2016) 714–735.